ACS OMEGA

http://pubs.acs.org/journal/acsodf

Article

Friction Dynamics of Foams under Nonlinear Motion

Kei Kikuchi, Akari Iwasawa, Mitsuki Omori, Hiroyuki Mayama, and Yoshimune Nonomura*

Cite This: *ACS Omega* 2022, 7, 16515−16523

Read Online

ACCESS | Metrics & More | Article Recommendations | Supporting Information

ABSTRACT: Foams are viscoelastic soft materials with complex mechanical properties. Here, we evaluated the friction dynamics of foams between acrylic plates using a sinusoidal motion friction evaluation system and we found some interesting characteristics under accelerated conditions. On a typical solid surface, a symmetrical friction profile, in which static and kinetic frictions are observed, is obtained under reciprocating nonlinear motion. Meanwhile, significant lubricant effects and velocity-dependent friction profiles without static friction were observed in foams. The friction force in foams increased in proportion to the power of velocity, with a power index of <1. These characteristic and dynamic phenomena in foams were observed in this study. They had been caused by the formation of a thick lubricant film and various dissipative modes including surfactant diffusion, viscous dissipation, and wall slip of bubbles. Moreover, the addition of a thickener increased the friction force and the delay time of friction response and improved the foam durability against normal force and shear. These findings are useful for understanding dynamic phenomena in soft materials.

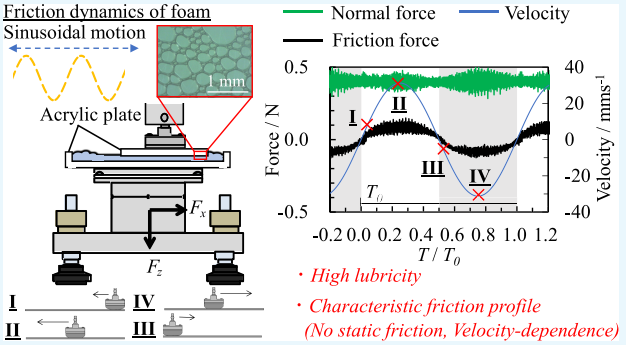

INTRODUCTION

Foams are viscoelastic soft materials with complex mechanical properties. They have both solid- and liquid-like mechanical properties. Although the dispersion of bubbles in the liquid phase can raise the viscosity of the fluid and give it solid-like mechanical properties, foams flow like a liquid when a certain strain is applied: when the strain applied to the foam reaches the yield value, the storage modulus G' decreases and the loss modulus G'' increases.[1−3] Géminard *et al.* evaluated the mechanical response of foams to large-amplitude shear.[4] During the reciprocating motion, a limit cycle where the sign of stress was reversed between the outward and homeward directions was observed. The maximum stress became constant when the maximum strain was exceeded: the bubbles deform and rearrange when foams are sheared with large amplitude. In addition, the viscous stress increases in proportion to the power of the capillary number Ca*, where $Ca^* = (\mu V_0/\sigma)$.[5−11] The parameters are the viscosity of the liquid, μ; the relative velocity between the foam and wall, V_0; and the surface tension, σ. The power index, n, is <1, indicating that the effective viscous coefficient decreases with increasing shear rate. These results suggest that foams have various modes of energy dissipation. The relationship between viscous stress and shear rate follows a different scaling law in the cases of synthetic surfactants, which form relatively fluid interfaces, and soaps, which form rigid interfaces: the latter produces significantly higher viscous stress.

Although many researchers have evaluated the friction and rheological properties of foams, almost all evaluations were performed under decompression, uniform motion, or small strain conditions. However, under compressive conditions and nonlinear motion, the characteristic frictional phenomena of foams are expected to occur. Stribeck showed that the state of lubrication between solid surfaces depends on the shear rate, the viscosity of the lubricant, and the vertical force.[12] It is difficult to explain friction phenomena on soft materials based on the classical theory because they are complicated. For example, Kurokawa *et al.* observed that the friction force on the gel surface changed nonlinearly with velocity in the transition process from elastic friction to fluid lubrication.[13] In addition, the effective viscous coefficient of foam decreases with increasing velocity. We have developed a friction evaluation system in which a contact probe moves in a sinusoidal motion and proposed the two-phase nonlinear model to reflect the viscoelastic properties in the friction model.[14−16] The model reflects the effects of velocity, acceleration, stiffness, viscosity, and vertical loading. Shinomiya *et al.* found characteristic friction phenomena between flat agar gel surfaces: an asymmetric friction profile with a lubrication state was observed when gels were rubbed for a shorter time than the relaxation time.[17]

Received: February 2, 2022
Accepted: April 21, 2022
Published: May 3, 2022

Table 1. Composition and Geometrical and Physical Properties of Surfactant Aqueous Solutions

	composition/wt %						
sample	SDS	myristic acid	cationaized cellulose	water	viscosity/mPa s	porosity	diameter/nm
1	19	1.0	0.0	80.0	5.21 ± 0.11	0.91 ± 0.01	0.16 ± 0.12
2			0.1	79.9	8.21 ± 0.16	0.89 ± 0.01	0.11 ± 0.10
3			0.5	79.5	31.0 ± 0.06	0.74 ± 0.03	0.08 ± 0.05

In this study, the friction dynamics of foams between acrylic plates was evaluated using a sinusoidal motion friction evaluation system to show their behavior under dynamic conditions. To the foaming formulation containing sodium dodecyl sulfate (SDS) and myristic acid, 0−0.5 wt % cationized cellulose was added to control the viscosity of the surfactant solution. SDS and myristic acid are widely used foaming agents in many fields. In particular, an SDS/myristic acid mixed system has been found to form an elastic and stable foam film.[8] We analyzed the relationship between the friction force and velocity/normal force and the effect of the viscosity of the surfactant solution. In addition to foams, we evaluated the friction dynamics of surfactant aqueous solutions before foaming to clarify the effects of air bubbles and surfactant molecules. The present findings are useful not only for understanding the dynamic phenomena that occur on the surface of soft materials but also for elucidation of the texture recognition mechanism.

EXPERIMENTAL SECTION

Materials. SDS [$CH_3(CH_2)_{11}OSO_3Na$, 98%] was purchased from Fujifilm Wako Pure Chemical Industries, Ltd. (Osaka, Japan). Myristic acid [C14:0 fatty acid, $CH_3(CH_2)_{12}COOH$, 98%] and cationized cellulose [Poise C-60H, Polyquaternium-10] were obtained from Kao Corporation (Tokyo, Japan). Water was purified using the Demi-Ace Model DX−15 demineralizer (Kurita Water Industries Ltd., Tokyo, Japan). To prepare an aqueous surfactant solution, a surfactant mixture of SDS/myristic acid (95/5, wt/wt), thickener (cationized cellulose), and deionized water were mixed and heated at 80 °C with stirring at 500 rpm by a magnetic stirrer for 1 h. The resulting solution was left for 1 h at 25 °C prior to use. A foam was prepared in the air by stirring the aqueous surfactant solution for 30 s using a rotational stirrer model Creamer Cute from HARIO Co., Ltd. (Tokyo, Japan).

Table 1 shows the composition, viscosity of the surfactant aqueous solutions, porosity of foams, and diameter of bubbles. Sample 1 is the surfactant aqueous solution containing 19 wt % SDS and 1 wt % myristic acid. Solutions 2 and 3 containing 0.1 wt % and 0.5 wt % cationized cellulose were prepared to show the effect of the thickener on the friction. The mixed state of these solutions was observed using a polarizing microscope (XTP-11, Nikon Corporation, Tokyo, Japan). The viscosity was measured using a rotational viscometer (ViscoQC300, Anton Paar GmbH, Graz, Austria). The measurement conditions were as follows: coaxial cylinder type; spindle CC18; sample volume = 6.4 mL; shear rate = 39 s^{-1}. The viscosities, η, of the surfactant aqueous solutions 1−3 were 5.21 ± 0.11, 8.21 ± 0.16, and 31.0 ± 0.06 mPa s, respectively. In the preliminary test, since the measurements were made after preshearing at high speed, no significant velocity dependence on viscosity was observed.

The porosity, ε, which was calculated using eq 1, was evaluated immediately after foaming.

$$\varepsilon = (Z - z)/Z \quad (1)$$

Here, Z and z are the total volume of foam and the volume of the liquid phase, respectively. We weighed a foam in a Petri dish. The volume of the foam was measured beforehand. We then estimated the volume (z) with the assumption that the densities of the air and surfactant aqueous solution were 0 and 0.99 g mL^{-1}, respectively. The porosity, ε, of foams 1−3 were 0.91 ± 0.01, 0.89 ± 0.01, and 0.74 ± 0.03, respectively. In addition, the Feret diameter of the bubbles was measured when the foam was sandwiched between acrylic plates. The average particle sizes of foams 1−3 were 0.16 ± 0.12, 0.11 ± 0.10, and 0.08 ± 0.05 mm, respectively.

Measurements. The friction of foam between two acrylic plates (upper side: 70 × 40 × 5 mm^3, lower side: 120 × 50 × 3 mm^3) was evaluated using the sinusoidal motion friction evaluation system (Figure 1). A sinusoidal motion was

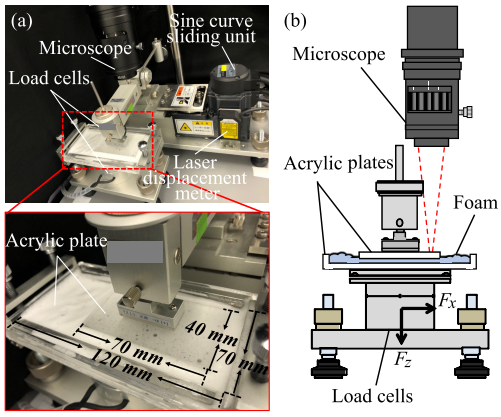

Figure 1. Sinusoidal motion friction evaluation system. (a) Overall picture. (b) Conceptual diagram.

achieved through the Scotch yoke mechanism. The evaluation method has been reported previously.[14] The sliding velocity (V) under the sinusoidal movement was calculated using the stroke length (D), angular velocity (ω), and time (T) based on eq 2:

$$V = |D|\omega \cos \omega T. \quad (2)$$

Here, the friction conditions were as follows: D = ±15 mm; ω = 0.1, 1.0, and 2.1 rad s^{-1}; sampling interval = 20, 10, and 1 ms; and normal force W = 0.20, 0.39, 0.59, 0.98, and 1.47 N. The average sliding velocities for the angular velocity were 1 mm s^{-1} (0.1 rad s^{-1}), 10 mm s^{-1} (1.0 rad s^{-1}), and 20 mm s^{-1} (2.1 rad s^{-1}). The sampling period was determined so that 300 data points were collected per period. Since vertical load and velocity were expected to have significant effects on the friction dynamics, five and three conditions were selected.

Before an evaluation of friction, the lower acrylic plate was covered with a foam having a thickness of 3 mm. The upper acrylic plate was then placed on top of the foam. Each evaluation was conducted three times to verify the

https://doi.org/10.1021/acsomega.2c00677
ACS Omega 2022, 7, 16515−16523

repeatability. The foams were replaced for each assessment. All the described evaluations were performed at 25 ± 1 °C and 50 ± 5% relative humidity. In addition, the conditions of bubbles before and after friction evaluation were observed using a microscope (Hozan Tool Ind. Co., Ltd., Osaka, Japan). The occurrence frequency and average size of bubbles are described in Figures S1 and S2 in the Supporting information.

RESULTS AND DISCUSSION

Friction Profile of Foams. Figure 2 shows the temporal profiles of the normal force, sliding velocity, and friction force

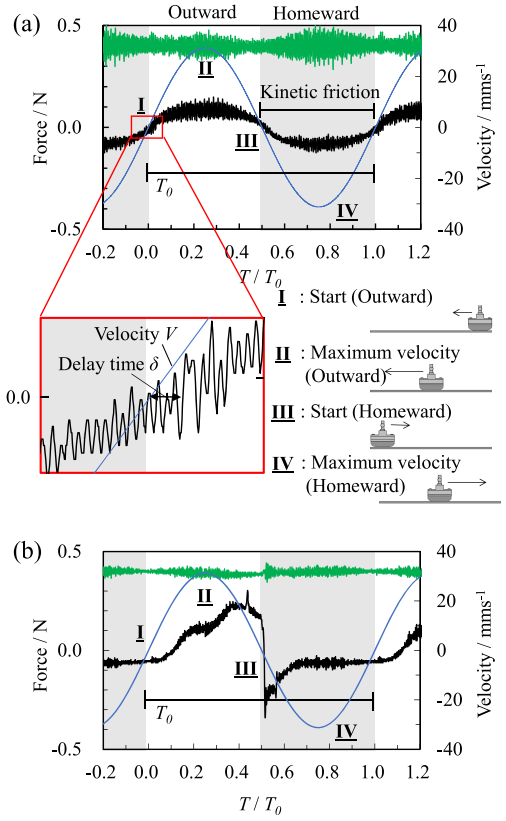

Figure 2. Temporal profile of the friction force (black line), velocity (blue line), and normal force (green line) at ω = 2.1 rad s^{-1} and W = 0.39 N. (a) Foam **2** and (b) surfactant aqueous solution **2**.

of the foam and the surfactant aqueous solution under sinusoidal motion: angular velocity ω = 2.1 rad s^{-1}, and normal force W = 0.39 N. The initial direction of movement of the contact probe and the opposite direction were defined as the outward and homeward directions, respectively. A velocity-dependent friction profile with no static friction was observed in the case of foam **2** (Figure 2a). The same behavior, in which the friction force increased with speed, was observed in the outward and homeward directions: vibration of the friction force was observed in the range of 0.05−0.11 N, and the friction force was 0.09 N at the maximum velocity V_{max} = 30 mm s^{-1}. In addition, a time lag in the response of the friction force to the movement of the contact probe was observed. The delay time (δ) was normalized by dividing with the friction time (T_0). The value was 0.012 for a 1-round trip. We observed that the δ was affected by various factors such as the hardness and thickness of the material and viscosity of the fluid.[16,18,19] Conversely, in the case of surfactant aqueous solution **2**, static friction and a sharp increase in friction force were observed (Figure 2b). In the outward direction, no static friction was observed, and the friction force increased to 0.25 N during the kinetic friction process. In the homeward direction, the static friction force was −0.34 N for static friction and −0.06 N during the kinetic friction process.

Figure 3 demonstrates the relationships between the friction coefficient and sliding velocity. In the present study, two types

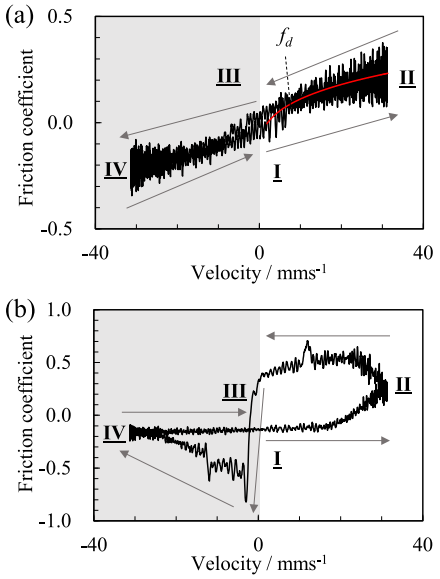

Figure 3. Relationship between friction coefficient and velocity at ω = 2.1 rad s^{-1} and W = 0.39 N. The red line indicates the fitting result. (a) Hydrodynamic stable pattern: foam **2**, (b) unstable pattern: surfactant aqueous solution **2**.

of friction profiles were observed. The features of each friction profile are as follows.

(a) Hydrodynamic stable pattern: In the case of foam **2** at ω = 2.1 rad s^{-1} and W = 0.39 N, a hydrodynamic stable pattern was observed on the first cycle, in which similar profiles were obtained during the outward and homeward processes (Figure 3a). Here, the friction coefficient increased with sliding velocity. At maximum velocity, V_{max} = 30 mm s^{-1}, the friction coefficient was 0.20.

(b) Unstable pattern: In the case of surfactant aqueous solution **2** at ω = 2.1 rad s^{-1} and W = 0.39 N, an unstable pattern was observed, in which static friction and a rapid increase in friction were observed (Figure 3b). In the outward direction, no static friction was observed, and the friction coefficient increased gradually. Here, the friction coefficient was 0.59 at V = 22.4 mm s^{-1}. In the homeward direction, static friction with a friction coefficient of −0.81 was observed at V = −2.92 mm s^{-1}. The friction coefficient decreased, and the kinetic friction with a friction coefficient of −0.15 was observed.

To our knowledge, a hydrodynamic stable pattern has not been observed on common solid surfaces. The tendency of the friction force to increase with speed suggests that the sliding state is in the fluid lubrication region. Here, the kinetic friction coefficient was approximated by the viscous friction model on the soft material surfaces.[14]

$$f_d = CV^N + f_c \quad (3)$$

https://doi.org/10.1021/acsomega.2c00677
ACS Omega 2022, 7, 16515−16523

where f_d is the kinetic friction coefficient and C is the viscous coefficient. f_c is the friction coefficient at $V = 0$ mm s^{-1}, and N is the power index. For example, eq 4 was obtained by substituting the friction data of foam **2** at $\omega = 2.1$ rad s^{-1} and $W = 0.39$ N.

$$f_d = 0.15V^{0.30} - 0.19 \quad (4)$$

C, f_c, N, and R^2 were 0.15, −0.19, 0.30, and 0.53, respectively. It is characteristic that N was as small as 0.3. In general, in the evaluation of Newtonian fluids in the fluid lubrication region, N is approximately 1; i.e., the friction coefficient increases in proportion to the velocity.[14]

Effects of the Normal Force and the Angular Velocity on Friction Force. Figure 4 and Table S1 show the relationship between the average friction force and the normal force. The average friction force is the average of the absolute value of the friction force for a cycle. In the case of foam **2**, the average friction forces at $\omega = 0.1$, 1.0, and 2.1 rad s^{-1} were 0.01, 0.05, and 0.06−0.07 N, respectively. The friction force did not depend on the normal force and increased with increasing sliding speed. In the case of $\omega = 2.1$ rad s^{-1} and $W =$ 1.47 N, the average friction coefficients of foams **1**−**3** were 0.03 ± 0.00, 0.05 ± 0.00, and 0.08 ± 0.00, respectively. Under high-load conditions, all friction coefficients were <0.1: foam showed a high-lubrication property. The friction coefficient increased as the amount of thickener added increased. The average friction coefficients of the surfactant aqueous solutions **1**−**3** under the same condition are 0.12 ± 0.04, 0.17 ± 0.00, and 0.05 ± 0.00, respectively (Table S2).

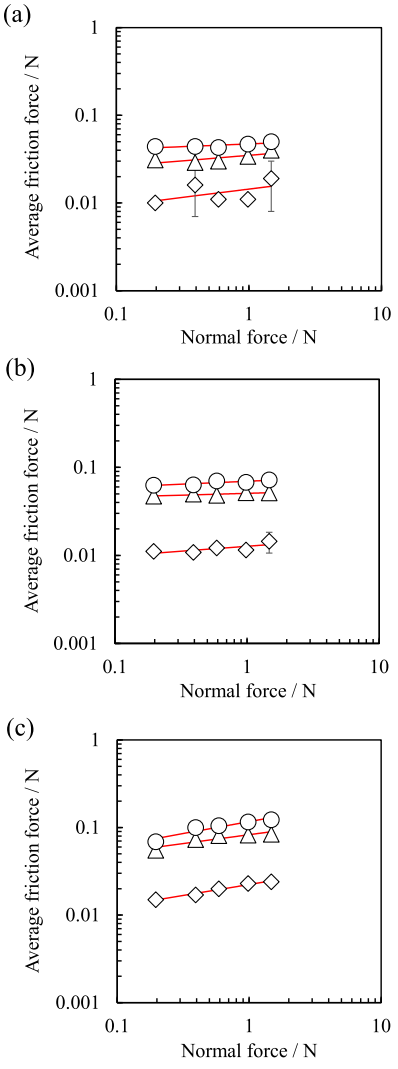

Figure 4. Average friction force at each normal force: $\omega = 0.1$ (rhombus), 1.0 (triangle), 2.1 rad s^{-1} (circle). (a−c) Foams **1**, **2**, and **3**.

The average friction force was analyzed on the basis of the power law, which was described using eq 5.

$$F = a\,W^n \quad (5)$$

where a and n are constants. If $n = 1$ and a is the friction coefficient, the relationship between F and W follows the Amontons−Coulomb law. Table S1 shows the values of a, n, and R^2. R^2 is the coefficient of determination, which represents the degree of dispersion when two variables are regressed by a straight line. In the case of foams, a and n were 0.013−0.117 and 0.043−0.273, respectively. The small n also suggests that the friction force is almost unaffected by the normal force and does not follow the Amontons−Coulomb law. Conversely, in the case of the surfactant aqueous solutions, n was 0.528−1.029, suggesting that the friction force increased with the normal force (Figure S3 and Table S2).

Effects of the Normal Force and Angular Velocity on Delay Time δ. Figure 5 shows the delay time, δ, for the first cycle. In the case of foam **2**, the delay times δ at $\omega = 0.1$, 1.0, and 2.1 rad s^{-1} were 0.023−0.032, 0.016−0.017, and 0.012−0.016, respectively. The time δ did not depend on the normal force and increased slightly as the sliding speed decreased. At $\omega = 2.1$ rad s^{-1} and $W = 0.39$ N, the delay times δ of foams **1**−**3** were 0.004 ± 0.004, 0.012 ± 0.003, and 0.011 ± 0.002, respectively. The lack of dependence on the normal force may be due to a thin foam film, small deformability of the bulk, and lubricity of the foam. The time δ of foam **1** was not significant, whereas that of foams **2** and **3** exceeded 0.01. In the case of surfactant solution, it was impossible to compare samples **1**−**3**, because the variation of the obtained data was extremely large (Figure S4 and Table S2).

Durability of Foams against Normal Force and Shear. Figure 6 shows the average friction force of foams in the 10 cycles of friction evaluation at $\omega = 1.0$ rad s^{-1} and $W = 0.98$ N. The open and closed circles suggest the conditions of hydrodynamic stable and unstable patterns, respectively. In the case of foam **1**, a hydrodynamic stable pattern was observed from the first cycle to the sixth cycle, whereas an unstable pattern was observed after that (Figure 6a). The average friction forces at the first and tenth cycles were 0.03 and 0.04 N, respectively. The friction force increased slightly from the seventh cycle where an unstable pattern was observed. Conversely, in the case of foam **2**, only a hydrodynamic stable pattern, whose average friction force was 0.05 N, was observed (Figure 6b). The average friction force found in foam **3** was 0.08 N, which also suggested a hydrodynamic stable pattern (Figure 6c). Representative images of bubbles in the foams are shown in Figure 7. Most of the bubbles in foam **1** collapsed after friction evaluation (Figure 7a-2). Meanwhile, many bubbles remained between the two acrylic plates in foams **2** and **3** (Figure 7b-2,c-2). These results suggest that an unstable pattern was observed when the acrylic plates come into contact with each other because the bubbles were collapsed.

https://doi.org/10.1021/acsomega.2c00677
ACS Omega 2022, 7, 16515−16523

We evaluated the number of cycles where an unstable pattern was observed to evaluate the foam durability against normal force and shear (Figure 8). In the case of foam **2**, a change in the friction profile was observed at [ω = 2.1 rad s^{-1}, W = 1.47 N] and [ω = 0.1 rad s^{-1}, W = 0.39−1.47 N]. Only a hydrodynamic condition was observed under other conditions. This result demonstrates that the acrylic plates come into contact under slow speed and high-load conditions. In the case of foam **1** without the thickener, the number of conditions in which the hydrodynamic stable pattern appeared was reduced, and the change in friction pattern was observed at a faster number of reciprocations. In the case of foam **3** with high thickener content, the number of conditions in which the hydrodynamic stable pattern appeared increased. Therefore, the addition of the thickener improved the durability against vertical force and shear. In the case of the surfactant aqueous solutions, an unstable pattern was observed under many conditions (Figure S5).

Lubrication Mechanism of Foam. The friction dynamics of foams between acrylic plates was systematically evaluated using a sinusoidal motion friction evaluation system to show their behavior under dynamic conditions. Here, we found three characteristics. The first is a viscous friction profile, in which static friction does not occur and the friction force increases with velocity. Foam showed a significant lubricant effect under high-load conditions: the friction coefficient was <0.1. Second, the friction coefficient increased in proportion to the power of the velocity: the power index N was <1. Finally, the addition of thickener to foam increased the friction force and the delay time of friction response and improved the foam durability against normal force and shear. These friction characteristics were different from those of the surfactant aqueous solution, which is a typical lubricant.

Now, we considered the lubrication effect of foam. In general, the friction phenomenon on a wet surface is analyzed using the Stribeck curve.[12] The lubrication state is distinguished on the basis of the relationship between the friction coefficient and the Sommerfeld number, S, which is defined using eq 6.

$$S = \frac{\eta \times V}{W} \tag{6}$$

When the viscosity of the lubricating film η and the sliding velocity V increase and the normal force W decreases, the number S increases. The lubrication condition changes from boundary to hydrodynamic lubrication. The lubrication state is assumed to be boundary or mixed lubrication in the case of the surfactant aqueous solution, while it is hydrodynamic lubrication in the case of the foam because the effective viscosity of the foam is high. Bubbles do not easily collapse under the compression condition if the foam is stabilized by elastic molecular films and the diffusion of surfactant molecules such as the Marangoni effect, which is the repair of a locally heterogenized membrane.[10,11,20−23]

Energy Dissipation. The present result that the friction force increased in proportion to the power of velocity is similar to that of previous studies. Denkov *et al.* evaluated the rheological properties of foam and proposed some theoretical models.[5,6,8−11] The viscous friction inside the foam was evaluated to analyze the stress, τ_V, based on the Herschel−Bulkley model (eq 7).[5] This model expresses the viscosity of a general non-Newtonian fluid and describes the shear behavior of a foam when bubbles do not slip on the surface of a frictional substrate.

$$\tau_V = \tau_0 + k_V \gamma^m, \tag{7}$$

where τ_0 is the elastic stress, k_V is the foam consistency, γ is the rate of shear deformation, and m is the power law index. For foam at air volume fraction Φ = 0.90, m was 0.25−0.42 and the effective viscous friction decreased as the shear rate increased.

In addition, the foam−wall friction was evaluated. This model describes the shearing phenomenon of a foam on a surface of a flat plate.[6] It evaluates the force dissipation in a thin film between the bubble and plate. In the case of a tangentially mobile bubble surface, the foam−wall friction, τ_W, is described using eq 8.

$$\tau_W \propto (\mathrm{Ca}^*)^{2/3}, \tag{8}$$

where Ca* is the capillary number, defined with the liquid viscosity, μ; relative velocity between foam and wall, V_0; and the surface tension, σ (eq 9).

$$\mathrm{Ca}^* = \mu V_0/\sigma \tag{9}$$

These results suggested that the viscous friction inside the foam τ_V and the foam−wall friction τ_W increase in proportion to the power of velocity.

The various dissipative modes of foam cause a decrease in the effective friction coefficient as sliding speed increases. It is possible that the viscous dissipation[5,24,25] and the dissipation related to surfactant diffusion affect the friction dynamics of foam[18−20] because a thick lubricating film was formed between the plates. In addition, the dissipation related to wall slip of bubbles is one of the most important modes because a smooth acrylic plate was used in this study. In general, a substrate with a rough surface is selected to minimize the effect of wall slip of a bubble when the rheological properties inside the foam are evaluated.[5]

Effect of the Addition of a Thickener. The frictional dynamics of the foam of the surfactant solution containing only SDS was almost the same as that of the surfactant solution **1** containing SDS and myristic acid (Figure S6−S8 and Table S3). However, as shown in Figures 4−8, the addition of a thickener caused obvious changes. The friction force of foam containing a thickener increased because the viscosity of the continuous phase affects the frictional force in the hydrodynamic lubrication state. The thickness of the lubricating film between the acrylic plates can be related to the delay time, δ. The friction response was delayed as the lubricating film increased. We considered that the durability of the foam was improved for the following reasons. The foam film stabilizes as the drainage rate of the liquid phase slows.[24,25] For charged thickeners, the electrostatic repulsion prevents thinning of the foam film.[26−30] In addition, the aggregation of a positively charged polymer and an anionic surfactant enhances the foam stability.[31−36]

Examination of the Temporal Profiles of Friction and Normal Forces. The temporal profile of the normal force of foam **2** in Figure 2a, in particular, appears to be chaotic patterns due to the fine oscillations shown in the inset and the periodic changes of the whole amplitudes of the normal force, which resemble a beating pattern. While analyzing temporal profiles to confirm the possibility of chaotic patterns, we discovered that the fine oscillations are caused by frictions between foams (Figures S9 and S10), and periodic changes are

https://doi.org/10.1021/acsomega.2c00677
ACS Omega 2022, 7, 16515−16523

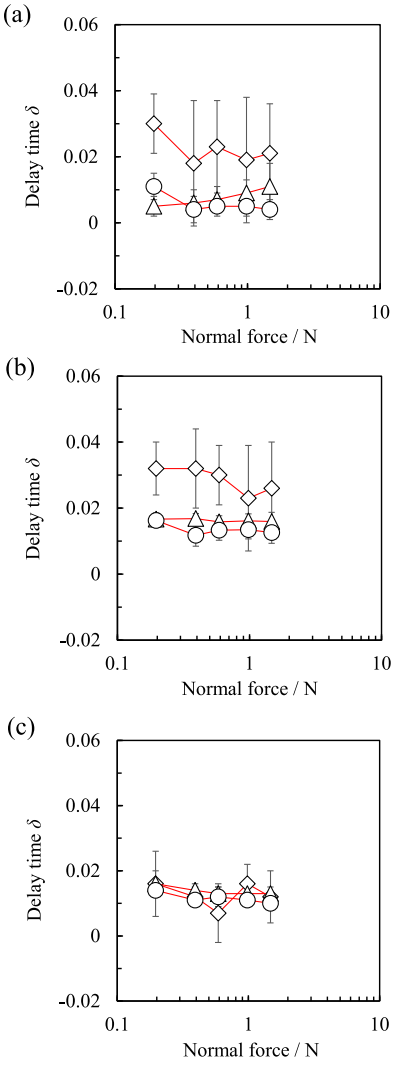

Figure 5. Delay time, δ, at each normal force: ω = 0.1 (rhombus), 1.0 (triangle), 2.1 rad s^{-1} (circle). (a–c) Foams **1**, **2**, and **3**.

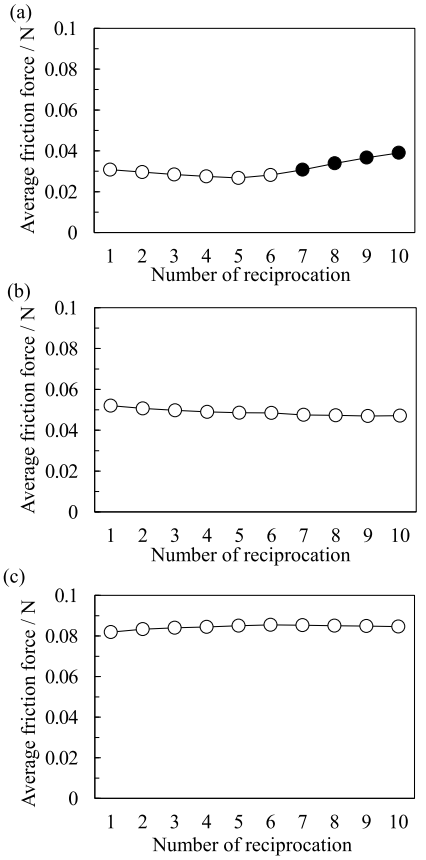

Figure 6. Relationship between the average friction force and the number of reciprocations obtained at ω = 1.0 rad s^{-1} and W = 0.98 N; hydrodynamic stable pattern (open circle) and unstable pattern (closed circle). (a–c) Foams **1**, **2**, and **3**, respectively.

strongly correlated with sinusoidal motion. The specifics have been omitted; see the Supporting information for more details.

A Molecular-Level Explanation for the Friction Behavior of Foam. We found that the prepared foam showed remarkable lubrication properties and low velocity dependence under a nonlinear motion. Furthermore, the stability of the foam was found to be dependent on the amount of thickener used. Our analyses have focused on the macroscopic scale phenomena, which we cannot explain at the molecular level. Therefore, we proposed a hypothesis based on previous reports. The foam-induced lubrication phenomenon can be explained by the adsorption of a surfactant to a substrate. Liu *et al.* used atomic force microscopy (AFM) and found that the adsorption of surfactants significantly reduced the frictional force on mica substrates.[37] Yamada and Israelachvili used a surface force apparatus to evaluate the friction and adhesion hysteresis of a monolayer of fluorosurfactant.[38] They suggested that the molecular groups at the surfaces rearranged slightly. This provided a smoother surface that reduced the force barrier for sliding. This mechanism was proposed to account for the abrupt load-induced reduction in friction, which was observed in fluorocarbon surfactant monolayers. Kamada *et al.* observed a

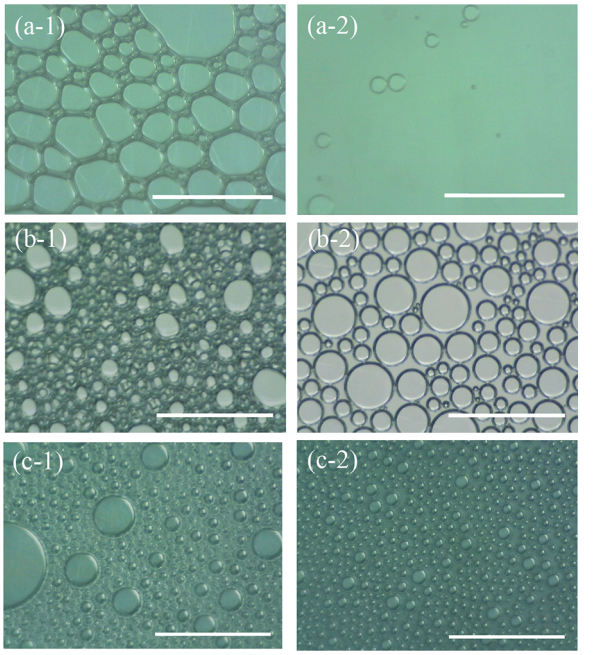

Figure 7. Images of bubbles at the friction interface. Scale bar indicates 1 mm. Conditions are ω = 1.0 rad s^{-1} and W = 0.98 N. Upper (a), middle (b), and lower (c) panels are for foams **1**, **2**, and **3**, respectively. Left panels: before evaluation and right panels: after evaluation.

https://doi.org/10.1021/acsomega.2c00677
ACS Omega 2022, 7, 16515–16523

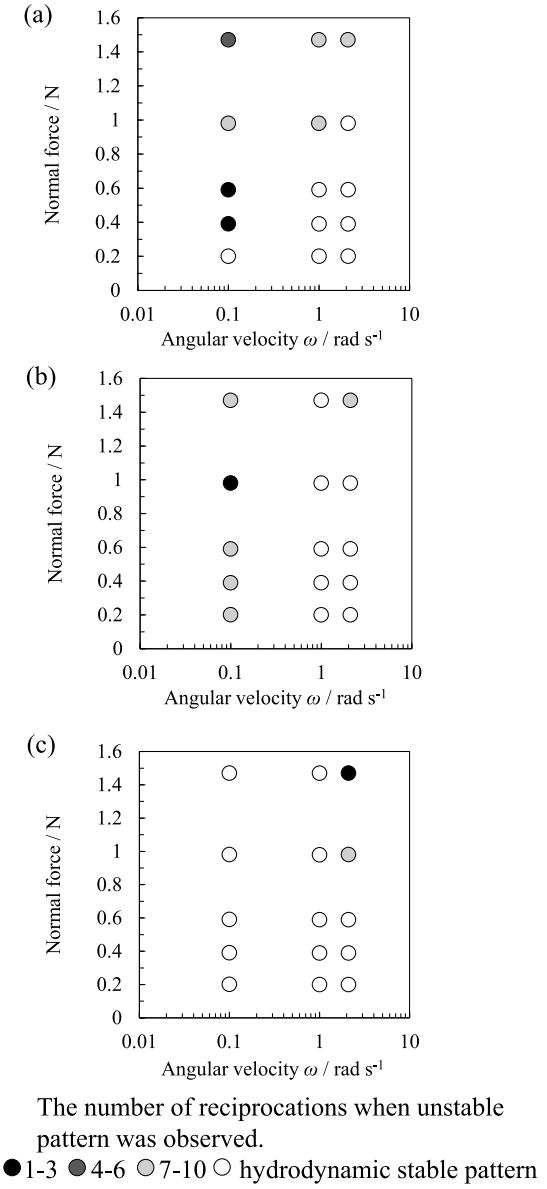

Figure 8. Dependence of normal force and angular velocity on the number of reciprocations when unstable pattern was observed. (a)–(c) Foams **1**, **2**, and **3**.

lubrication phenomenon between a hydrogel and solid surface due to the adsorption of surfactants.[39] Surfactants remained at the gel/surface interface, preventing the direct interfacial interaction between the sliding surfaces and thus significantly decreasing the frictional stress.

The very low velocity dependence observed in our foams was attributed to the energy dissipation in the foam film. Denkov *et al.* showed that the mechanical properties of a foam were dependent on the type of surfactant used.[10] The first class of surfactants are typical synthetic surfactants (e.g., SDS) that have low surface modulus and fast relaxation of surface tension. The second class of surfactants include fatty acid salts such as lauric and myristic acids, which have large surface areas and exhibit relatively high surface modulus and fast surface tension relaxation. Meanwhile, several reports have focused on the addition of thickeners to alter the conditions at the air–liquid interface. Addition of guar hydroxypropyltriammonium chloride to a surfactant solution significantly increased the yield stress of a foam. This resulted in a characteristic profile in the stress–shear rate curve.[40] These effects indicated the formation of polymer bridges between adjacent bubbles in a sheared foam. The effect of a polymer depends significantly on the head group of an anionic surfactant.[36] In foam generation, weakly interacting systems have provided significant benefits and synergistic effects. Strong interactions could be beneficial or detrimental to foam stability. These interactions depend strongly on a specific surfactant and/or a specific procedure for foam generation.

Furthermore, previous research on the Gibbs adsorption films formed by water-soluble surfactants at the air–liquid interface aids in understanding the mechanism of foam stability and energy dissipation. Surfactant molecule packing in the Gibbs adsorption membrane has a significant impact on the mechanical properties of the interfacial membrane and foam stability.[41] To put it another way, the aqueous SDS solution produced unstable foam, whereas the fatty acid–fatty alcohol mixture produced stable foam. This finding implies that the smaller the molecular occupied area at the interface, the harder the interface and the more stable the foam becomes. When air enters the surfactant solution, the micellar lifetime is also an important factor in foamability.[42] The foamability of aqueous surfactant solutions with a long micellar lifetime was the lowest.

Surfactant and polymer molecules form aggregates in water or at the air–water interface, influencing the foam's mechanical properties and stability. Between critical aggregation and critical micelle concentrations, the number of aggregates composed of SDS and cationic polymers increased significantly.[43] The strength of the surfactant–polymer interaction has a significant impact on foamability and foam stability. For example, a strong interaction between SDS and the cationic polymer resulted in high foam stability but poor foamability.[35] According to a recent study, adsorption to the interface of this surfactant–polymer complex occurs in two steps.[44] In the case of a two-step adsorption–equilibration, the initial stages involve the diffusion of kinetically trapped aggregates formed in the bulk to the interface followed by their dissociation and spreading at the interface.

The findings of foam flows and deformations can provide information on the mechanism of energy dissipation. Although foams are only made up of Newtonian fluids, foam flow follows nonlinear laws.[45] This can be caused by nonaffine deformations of the disordered bubble packing or by a coupling between the surface flow in the surfactant monolayers and the bulk liquid flow in the films, channels, and nodes. Cantat *et al.* conducted experiments that demonstrated that dissipation in foam flowing through a narrow rectangular channel is dominated by dissipation associated with plateau borders sliding over the channel walls.[46] This implies that film deposition/detachment at the walls is the primary dissipation mechanism. As a result, they have provided a detailed characterization of the dissipation processes relevant to quasi-planar rheological experiments. They recently monitored the evolution of the local flow velocity, film thickness, and surface tension of a five-film assembly induced by different controlled deformations and discovered that the majority of the dissipation is localized in the domains of menisci.[47]

CONCLUSIONS

In this study, we evaluated the effects of sliding velocity and normal force on the friction dynamics of foam using a friction

https://doi.org/10.1021/acsomega.2c00677
ACS Omega 2022, 7, 16515–16523

evaluation system, which used sinusoidal motion to find some characteristics of soft materials. A velocity-dependent symmetric friction profile without static friction was observed in foam, which showed a high-lubrication property under high-load conditions. The lubrication state becomes hydrodynamic lubrication because the bubbles stabilized by the surfactant support the normal force and form a thick lubricating film. Second, the friction coefficient increased in proportion to the power of velocity, and the power index N was <1. The various dissipative modes of foam cause a decrease in the effective friction coefficient as sliding speed increases. In the case of the surfactant aqueous solution, which is a typical lubricant, such friction characteristics were not observed. Moreover, the addition of thickener increased the friction force and the delay time of friction response and improved the foam durability against normal force and shear. This study revealed the friction dynamics of foam under a nonlinear motion, which can potentially elucidate the complex mechanical properties of colloidal dispersions and foams. In addition, it will be useful not only for the development of foam formulations such as foods and cosmetics but also for understanding the arousal mechanism of tactile texture.

■ ASSOCIATED CONTENT

Supporting Information

The Supporting Information is available free of charge at https://pubs.acs.org/doi/10.1021/acsomega.2c00677.

Details of the mixed state of emulsions; details of adhesion force evaluation system; parameters of friction and adhesion properties of emulsions (PDF)

■ AUTHOR INFORMATION

Corresponding Author

Yoshimune Nonomura − *Department of Biochemical Engineering, Graduate School of Science and Engineering, Yamagata University, Yonezawa 992-8510, Japan;* orcid.org/0000-0003-0461-124X; Phone: +81-238-26-3164; Email: nonoy@yz.yamagata-u.ac.jp; Fax: +81-238-26-3414

Authors

Kei Kikuchi − *Department of Biochemical Engineering, Graduate School of Science and Engineering, Yamagata University, Yonezawa 992-8510, Japan*

Akari Iwasawa − *Department of Biochemical Engineering, Graduate School of Science and Engineering, Yamagata University, Yonezawa 992-8510, Japan*

Mitsuki Omori − *Department of Biochemical Engineering, Graduate School of Science and Engineering, Yamagata University, Yonezawa 992-8510, Japan*

Hiroyuki Mayama − *Department of Chemistry, Asahikawa Medical University, Asahikawa 078-8510, Japan*

Complete contact information is available at: https://pubs.acs.org/10.1021/acsomega.2c00677

Notes

The authors declare no competing financial interest.

■ ACKNOWLEDGMENTS

This study was supported by a Grant-in-Aid for Scientific Research (C) (grant no. 20K12018) from the Ministry of Education, Culture, Sports, Science and Technology, Japan (MEXT).

■ REFERENCES

(1) Saint-Jalmes, A.; Durian, D. J. Vanishing elasticity for wet foams: Equivalence with emulsions and role of polydispersity. *J. Rheol.* **1999**, *43*, 1411−1422.

(2) Herzhaf, B.; Kakadjian, S.; Moan, M. Measurement and modeling of the flow behavior of aqueous foams using a recirculating pipe rheometer. *Colloids Surf., A* **2005**, *263*, 153−164.

(3) Marmottant, P.; Graner, F. An elastic, plastic, viscous model for slow shear of a liquid foam. *Eur. Phys. J. E: Soft Matter Biol. Phys.* **2007**, *23*, 337−347.

(4) Géminard, J.-C.; Pastenes, J. C.; Melo, F. Foam rheology at large deformation. *Phys. Rev. E* **2018**, *97*, No. 042601.

(5) Denkov, N. D.; Subramanian, V.; Gurovich, D.; Lips, A. Wall slip and viscous dissipation in sheared foams: Effect of surface mobility. *Colloids Surf., A* **2005**, *263*, 129−145.

(6) Denkov, N. D.; Tcholakova, S.; Golemanov, K.; Subramanian, V.; Lips, A. Foam−wall friction: Effect of air volume fraction for tangentially immobile bubble surface. *Colloids Surf., A* **2006**, *282-283*, 329−347.

(7) Terriac, E.; Etrillard, J.; Stone, I. C. Viscous force exerted on a foam at a solid boundary: influence of the liquid fraction and of the bubble size. *Europhys. Lett.* **2006**, *74*, 909.

(8) Golemanov, K.; Denkov, N. D.; Tcholakova, S.; Vethamuthu, M.; Lips, A. Surfactant Mixtures for Control of Bubble Surface Mobility in Foam Studies. *Langmuir* **2008**, *24*, 9956−9961.

(9) Tcholakova, S.; Denkov, N. D.; Golemanov, K.; Ananthapadmanabhan, K. P.; Lips, A. Theoretical model of viscous friction inside steadily sheared foams and concentrated emulsions. *Phys. Rev. E* **2008**, *78*, No. 011405.

(10) Denkov, N. D.; Tcholakova, S.; Golemanov, K.; Ananthpadmanabhan, K. P.; Lips, A. The role of surfactant type and bubble surface mobility in foam rheology. *Soft Matter* **2009**, *5*, 3389−3408.

(11) Mitrinova, Z.; Tcholakova, S.; Denkov, N.; Ananthapadmanabhan, K. P. Role of interactions between cationic polymers and surfactants for foam properties. *Colloids Surf., A* **2016**, *489*, 378−391.

(12) Mortier, R. M.; Fox, M. F.; Orszulik, S. T. *Chemistry and Technology of Lubricants*; 3rd ed.; Springer: Berlin, 2010, Chapter 3.

(13) Kurokawa, T.; Tominaga, T.; Katsuyama, Y.; Kuwabara, R.; Furukawa, H.; Osada, Y.; Gong, J. P. Elastic− Hydrodynamic Transition of Gel Friction. *Langmuir* **2005**, *21*, 8643−8648.

(14) Aita, Y.; Asanuma, N.; Takahashi, A.; Mayama, H.; Nonomura, Y. Nonlinear Friction Dynamics on Polymer Surface under Accelerated Movement. *AIP Adv.* **2017**, *7*, No. 045005.

(15) Aita, Y.; Asanuma, N.; Mayama, H.; Nonomura, Y. Sliding Profile and Energy at Static Friction between Polymer Surfaces. *Chem. Lett.* **2018**, *47*, 767−769.

(16) Asanuma, N.; Aita, Y.; Nonomura, Y. Tactile Texture of Cosmetic Sponges and Their Friction Behavior under Accelerated Movement. *J. Oleo Sci.* **2018**, *67*, 1117−1122.

(17) Shinomiya, K.; Mayama, H.; Nonomura, Y. Anomalous Friction between Agar Gels under Accelerated Motion. *Langmuir* **2018**, *34*, 12723−12729.

(18) Shinomiya, K.; Okawara, H.; Kikuchi, K.; Mayama, H.; Nonomura, Y. Friction Dynamics of Hydrogel Substrates with a Fractal Surface: Effects of Thickness. *ACS Omega* **2020**, *5*, 16406−16412.

(19) Kikuchi, K.; Mayama, H.; Nonomura, Y. Nonlinear Friction Dynamics of Oil-in-Water and Water-in-Oil Emulsions on Hydrogel Surfaces. *Langmuir* **2021**, *37*, 8045−8052.

(20) Ross, S.; Haak, R. M. Inhibition of foaming. IX. Changes in the rate of attaining surface tension equilibrium in solutions of surface-active agents on addition of foam inhibitors and foam inhibitors and foam stabilizer. *J. Phys. Chem.* **1958**, *62*, 1260−1264.

(21) Buzza, D. M. A.; Lu, C.-Y. D.; Cates, M. E. Linear Shear Rheology of Incompressible Foams. *J. Phys. II France* **1995**, *5*, 37−52.
(22) Durand, M.; Stone, H. A. Relaxation time of the topological T1 process in a two-dimensional foam. *Phys. Rev. Lett.* **2006**, *97*, 226101.
(23) Besson, S.; Debregeas, G. Statics and dynamics of adhesion between two soap bubbles. *Eur. Phys. J. E: Soft Matter Biol. Phys.* **2007**, *24*, 109−117.
(24) Brady, A. P.; Ross, S. The Measurement of Foam Stability. *J. Am. Chem. Soc.* **1944**, *66*, 1348−1356.
(25) Miles, G. D.; Shedlovsky, L.; Ross, S. Foam Drainage. *J. Phys. Chem.* **1945**, *49*, 93−107.
(26) Bergeron, V.; Radke, C. J. Equilibrium Measurements of Oscillatory Disjoining Pressures in Aqueous Foam Films. *Langmuir* **1992**, *8*, 3020−3026.
(27) Pugh, R. J. Foaming, foam films, antifoaming and defoaming. *Adv. Colloid Interface Sci.* **1996**, *64*, 67−142.
(28) Mysels, K. J.; Jones, M. N. Direct measurement of the variation of double-layer repulsion with distance. *Discuss. Faraday Soc.* **1996**, *42*, 42−50.
(29) Anachkov, S. E.; Danov, K. D.; Basheva, E. S.; Kralchevsky, P. A.; Ananthapadmanabhan, K. P. Determination of the aggregation number and charge of ionic surfactant micelles from the stepwise thinning of foam films. *Adv. Colloid Interface Sci.* **2012**, *183-184*, 55−67.
(30) Petkova, B.; Tcholakova, S.; Chenkova, M.; Golemanov, K.; Denkov, N.; Thorley, D.; Stoyanov, S. Foamability of aqueous solutions: Role of surfactant type and concentration. *Adv. Colloid Interface Sci.* **2020**, *276*, 102084.
(31) Goddard, E. D. Polymer/Surfactant Interaction Its Relevance to Detergent Systems. *J. Am. Oil Chem. Soc.* **1994**, *71*, 1−16.
(32) Bergeron, V.; Langevin, D.; Asnacios, A. Thin-Film Forces in Foam Films Containing Anionic Polyelectrolyte and Charged Surfactants. *Langmuir* **1996**, *12*, 1550−1556.
(33) Bhattacharyya, A.; Monroy, F.; Langevin, D.; Argillier, J. -F. Surface Rheology and Foam Stability of Mixed Surfactant-Polyelectrolyte Solutions. *Langmuir* **2000**, *16*, 8727−8732.
(34) Ropers, M. H.; Novales, B.; Boue, F.; Axelos, M. A. V. Polysaccharide/Surfactant Complexes at the Air-Water Interface -Effect of the Charge Density on Interfacial and Foaming Behaviors. *Langmuir* **2008**, *24*, 12849−12857.
(35) Petkova, R.; Tcholakova, S.; Denkov, N. D. Foaming and Foam Stability for Mixed Polymer−Surfactant Solutions: Effects of Surfactant Type and Polymer Charge. *Langmuir* **2012**, *28*, 4996−5009.
(36) Petkova, R.; Tcholakova, S.; Denkov, N. D. Role of polymer−surfactant interactions in foams: Effects of pH and surfactant head group for cationic polyvinylamine and anionic surfactants. *Colloids Surf., A* **2013**, *438*, 174−185.
(37) Liu, Y.; Evans, D. F.; Song, Q.; Grainger, D. W. Structure and Frictional Properties of Self-Assembled Surfactant Monolayers. *Langmuir* **1996**, *12*, 1235−1244.
(38) Yamada, S.; Israelachvili, J. Friction and Adhesion Hysteresis of Fluorocarbon Surfactant Monolayer-Coated Surfaces Measured with the Surface Forces Apparatus. *J. Phys. Chem. B* **1998**, *102*, 234−244.
(39) Kamada, K.; Furukawa, H.; Kurokawa, T.; Tad, T.; Tominaga, T.; Nakano, Y.; Gong, J. P. Surfactant-induced Friction Reduction for Hydrogels in the Boundary Lubrication Regime. *J. Phys.: Condens. Matter* **2011**, *23*, 284107.
(40) Politova, N.; Tcholakova, S.; Golemanov, K.; Denkov, N. D.; Vethamuthu, M.; Ananthapadmanabhan, K. P. Effect of Cationic Polymers on Foam Rheological Properties. *Langmuir* **2012**, *28*, 1115−1126.
(41) Shah, D. O.; Djabbarah, N. F.; Wasan, D. T. A Correlation of Foam Stability with Surface Shear Viscosity and Area per Molecule in Mixed Surfactant Systems. *Colloid Polym. Sci.* **1978**, *256*, 1002−1008.
(42) Oh, S. G.; Shah, D. O. Relationship between Micellar Lifetime and Foamability of Sodium Dodecyl Sulfate and Sodium Dodecyl Sulfate/1-Hexanol Mixtures. *Langmuir* **1991**, *7*, 1316−1318.
(43) Staples, E.; Tucker, I.; Penfold, J.; Warren, N.; Thomas, R. K.; Taylor, D. J. F. Organization of Polymer-Surfactant Mixtures at the Air-Water Interface: Sodium Dodecyl Sulfate and Poly-(dimethyldiallylammonium chloride). *Langmuir* **2002**, *18*, 5147−5153.
(44) Akanno, A.; Guzmán, E.; Fernández-Peña, L.; Llamas, S.; Ortega, F.; Rubio, R. G. Equilibration of a Polycation−Anionic Surfactant Mixture at the Water/Vapor Interface. *Langmuir* **2018**, *34*, 7455−7464.
(45) Cohen-Addad, S.; Höhler, R.; Pitois, O. Flow in Foams and Flowing Foams. *Annu. Rev. Fluid Mech.* **2013**, *45*, 241−267.
(46) Cantat, I.; Kern, N.; Delannay, R. Dissipation in Foam Flowing through Narrow Channels. *Europhys. Lett.* **2004**, *65*, 726−732.
(47) Bussonnière, A.; Cantat, I. Local Origin of the Visco-elasticity of a Millimetric Elementary Foam. *J. Fluid Mech.* **2021**, *922*, A25.

https://doi.org/10.1021/acsomega.2c00677
ACS Omega 2022, 7, 16515−16523